Austempering kinetics of a ductile iron

M. Pellizzari, C. Menapace, G. Straffelini, M. Cazzolli, M. Dal Molin, F. Vettore, E. Veneri

The austempering kinetics of a ductile iron (ADI) was studied by means of dilatometry. Small samples (10mm length, 4mm diameter) were austenitized between 850-900°C and austempered at different temperatures in the range 320-370°C. The austenite decomposition to form acicular ferrite and Carbon enriched austenite is evidenced by a net expansion which follows the typical kinetics of diffusional transformations, described by the JMA equation x(t)=1-exp(-(kt)n). The activation energy was calculated assuming fixed stages of transformation, namely 10 and 90% at different austempering temperatures. At the lowest austenitizing temperature (850°C) the transformation may be described by a single value of the activation energy (23,95 kJ/mol). On the other side, at 900°C the kinetics showed an influence of the austempering temperature: in the lowest temperature range the activation energy was in the same range of that calculated at 850°C (26,07 kJ/mol), whilst in the highest one it was considerably lower (6,2 KJ/mol). This behavior could be correlated to the coarser ausferrite microstructure arising from high temperature austenitizing and the different carbon redistribution during isothermal treatment.

KEYWORDS: DUCTILE IRON - AUSTEPERING - AUSFERRITE - ACTIVATION ENERGY

INTRODUCTION

Austempered ductile iron (ADI) has become a suited alternative of steel in many important applications [1,2,3]. The unique combination of high strength and toughness, given by the ausferritic microstructure, favored the use of lower hardness grades (eg. ADI JS/800-10 and JS/1050-6) for fatigue purposes on planet carriers also with solid shaft, hubs, suspension arms, steering knuckles and higher hardness grades (ADI JS/1200-3, JS/1400-1, HBW450 and ADIWR$_{PAT}$) for construction, mining and railway application when wear resistance is required.

The ausferrite microstructure is given by ferritic bainite plates and C-enriched austenite. It is obtained after austenitizing and isothermal holding in salt bath at temperature between 250 and 400°C, by means of the following transformation:

I) $$\gamma \rightarrow \alpha + \gamma_{HC}$$

The parent austenite decomposes into ferrite and High Carbon (HC) asutenite, which does not turn into martensite during cooling, due to proper stabilization. Reaction (I) characterizes the first stage of the austempering process and, in order to get the benefits listed above, it is suggested that it goes to completion. In other words, the presence of unreacted austenite needs to be avoided. On the other side, too long permanence and/or excessive soaking temperature may lead to a second reaction (II) involving the decomposition of austenite into thermodynamically more stable ferrite and carbides

II) $$\gamma_{HC} \rightarrow \alpha + \text{carbides}$$

known as the second austempering stage. The precipitation of carbides reduces the properties of ADI. Therefore, it is important to select the proper processing parameters to join the so called processing window, i.e. the time interval ranging from the end of the first stage and the start of the second one [4]. Many papers is literature deal with correlations between processing parameters and chemical composition, in view of the different influence exerted by different alloying elements on the width of the window. Most of papers are focused on the study of the transformation kinetics, based on microstructural and Xray diffraction investigation on samples obtained from interrupted austempering [4,5,6]. Dilatometry was seldom used to approach this study, even if some interesting benefits are associated to the use of this experimental technique. Fras et. al. correlated the time required to achieve the final stable dimension of dilatometric sample to the C saturation of austenite during the austenizing phase, showing that the process is faster in castings with thinner section, because of the higher graphite nodule density [7]. The same authors further demonstrate that the expansion associated to transformation (I) becomes higher at low austempering temperature, due to the increasing driving force and that the incubation time for the nucleation of ferrite accordingly increases. Hardness data well fitted with length change signals, confirming the suitability of dilatometry to achieve a large number of information by means of a considerably lower

M. Pellizzari, C. Menapace, G. Straffelini, M. Cazzolli, M. Dal Molin
University of Trento (Italy)

F. Vettore, E. Veneri
Zanardi Fonderie S.p.A., Minerbe (VR) (Italy)

number of tests. Cisneros-Guerrero also proposed dilatometry as a useful tool to determine the processing window of ADI [8]. Pérez et. al. studied the austempering kinetics of ductile iron showing that reaction (I) under isothermal condition may be described by a Johnson-Mehl-Avrami equation

(1) $$X(t) = 1 - \exp[-(kT)^n]$$

where $X(t)$ is the transformed austenite fraction, t is the time, k a reaction rate, T the absolute temperature and n the order of reaction [9]. The activation energy E was calculated, carrying out experiments at different austempering temperature. The activation energy changed with the austempering temperature, in the range 30.3-58.2 KJ/mol when the heat treatment was carried out between 370 and 420 C and 10.3-26.7 KJ/mol when the temperature varied from 270 to 350 C according to a different transformation mechanisms. Aim of this work is to study the transformation kinetics of an ADI by means of dilatometry. The influence of the austenitizing temperature will be considered.

MATERIALS AND EXPERIMENTAL PROCEDURES

The chemical composition of ductile iron studied in this work in reported in Table 1. According to ISO 17804 it corresponds to a standard grade JS/1050-6, showing a minimum strength of 1000MPa, a minimum yield strength of 700MPa, 5% rupture strain and 300-360HB hardness.

C	Mn	Si	Cr	Ni	Mo	V	Cu
3.41	0.44	2.68	0.02	0.04	0.01	0.002	0.82

Tab. 1 - Composition of ductile iron

Cylindrical dilatometric samples (4mm diameter, 10mm length) were extracted from thin section Y-block castings (10mm^2). Microstructural analysis was carried out by light optical microscopy after standard metallographic preparation by emery papers and polishing with diamond paste. Quantitative image analysis was carried out to determine the graphite nodules count and nodularity according to ASTM E2567 [10], obeying the minimum number of fields to consider minimum 500 nodules. Dilatometric tests were carried out by means of a Bähr dilatometer model 805A/D. Firstly, the critical cooling rate was determined. Samples were austenitized at two different temperatures (850 and 890°C for 15 minutes) by induction heating, rapidly cooled (50°C/s) to the austempering temperature (comprised between 290÷400°C) and isothermally hold until the first transformation stage was completed. A typical example (Figure 1) shows that the first stage of transformation is associated to a net expansion and that the end transformation corresponds to the achievement of the plateau in the deformation curve.

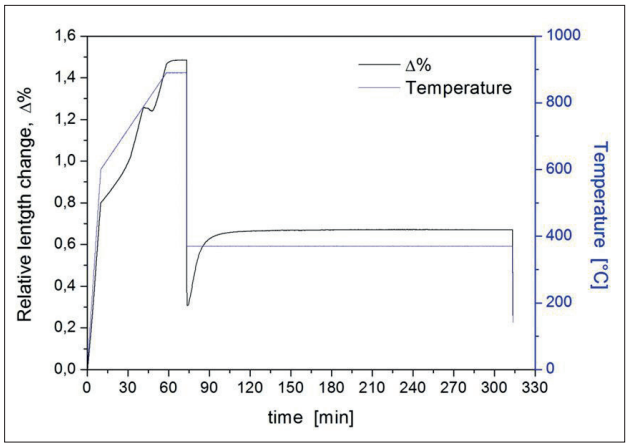

Fig. 1 - Austempering cycle showing the relative change in length as a function of temperature

The activation energy value related to the first austempering stage transformation was determined according to the formula method proposed in [11]

1) $$\ln(t_{f2} - t_{f1}) = \frac{E}{RT} + Cost$$

holding for under isothermal conditions, where t_{f1} e t_{f2} are the times corresponding to two fixed stages of transformation (0.1 e 0.9 transformed austenite), E is the activation energy (KJ/mol), R the gas constant (8,314 J/(mol*K) and T the absolute temperature (K).

The experimental points (t_{f2}-t_{f1}, T^{-1}) determined by different austempering temperatures were plotted and the activation energy calculated provided that they could be linearly interpolated.

RESULTS AND DISCUSSION

The microstructure of as-cast ductile iron evidences a very homogeneous distribution of graphite nodules, corresponding to a density of 588 nodules/mm^2, a nodularity of 90.9±1.8% and an average nodule size of 14.6µm. The iron matrix shows a bulls eye microstructure comprising a ferrite ring around graphite nodules and a perlite matrix. It is worth noting that a high nodule counts is representative of a high eutectic cell density and low microsegregation, i.e., a promising starting point for the study of the austempering kinetics.

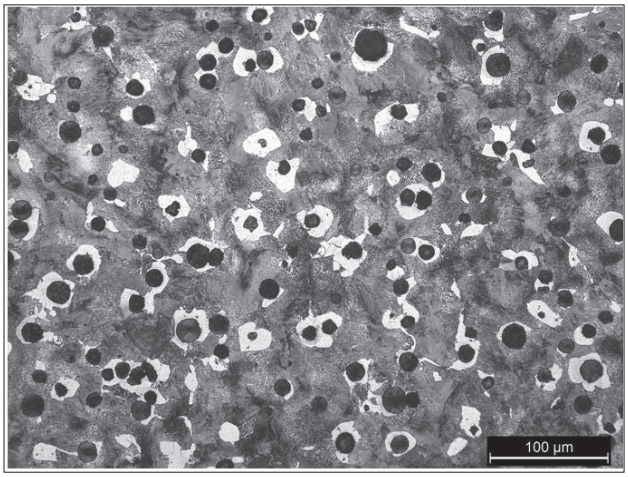

Fig. 2 - Microstructure of as-cast ductile iron

Table 2 reports the critical transformation points for the studied iron and the values of the critical cooling rate and M_s as a function of austenitizing temperature.

	Ac_1	Ac_3	$C.R._{crit}$	M_s
850°C	791±2	826±3	30°C/s	187±1°C
890°C			5°C/s	191±1°C

Tab. 1 - Ac_1, Ac_3, critical cooling rate and M_s values at different austenitizing temperatures

The M_s temperature does not show any appreciable influence of the austenitizing temperature. The critical cooling rates suggested the use of 50°C/s for the austempering experiments.

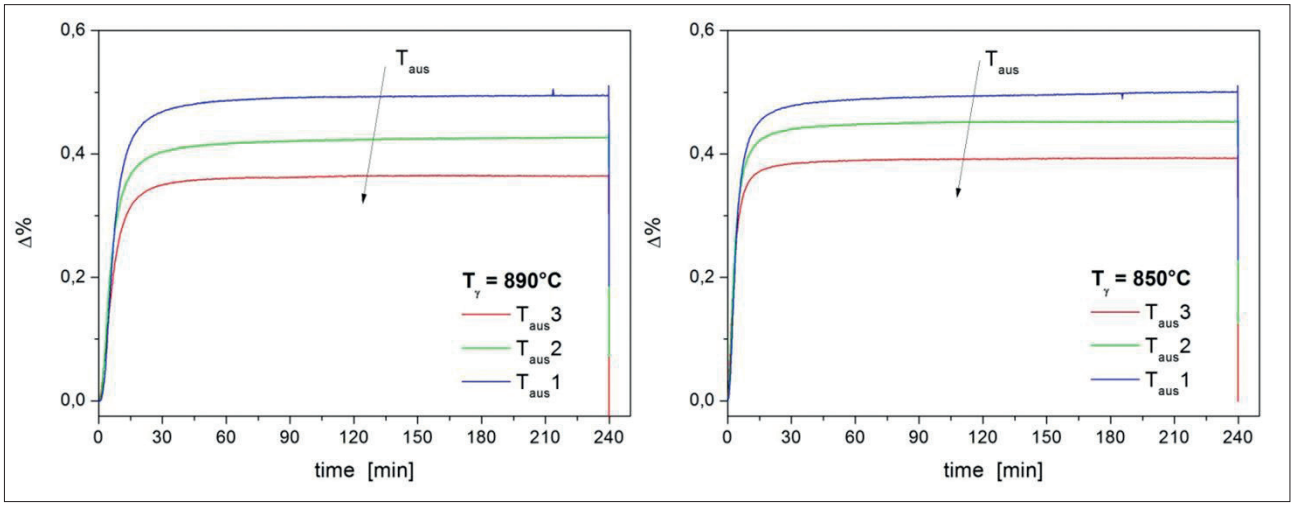

Fig. 3 - Relative change in length during austempering at different temperatures
a) T_γ=890°C, b) T_γ =850°C

The curves of relative change in length observed during austempering at different temperatures are shown in Figures 3a and 3b for the two austenitizing temperatures of 890 and 850°C, respectively.
At a first sight all curves confirm that after 4h present iron is still inside the processing window. Previous experiments confirmed that the decomposition of austenite into ferrite and carbides leads to a clear contraction, not observed here. A second consideration is that the net expansion due to the first stage transformation decreases by increasing austempering temperature. Moreover, the expansion is generally lower for samples austenitized at higher temperature (Figure 4).

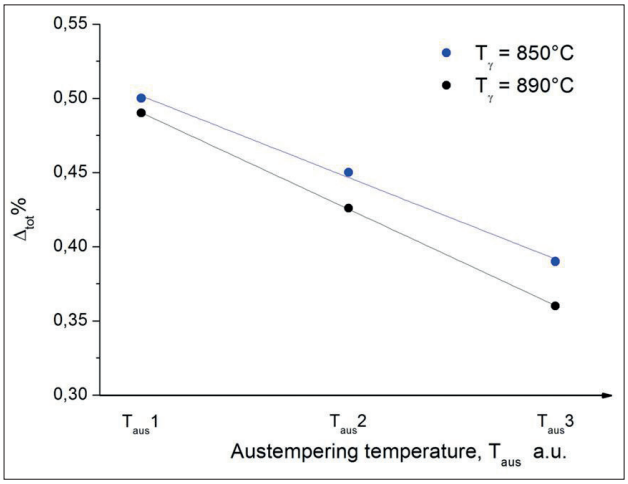

Fig. 4 - Relative change in length after austempering at different temperature

The first result can be explained by the higher driving force related to the decomposition of austenite at lower austempering temperature [12].
In fact, according to [6], the driving force is related to the difference between the C dissolved in parent austenite (C_γ^0) and that in transformed austenite, after reaction (i) (C_γ)

Driving force = C_γ-C_γ^0

which increases by reduced austempering temperature, due to the higher (C_γ). On the other hand, the second result is in agreement with the higher solubility of (C_γ^0) in austenite by increasing temperature, leading to higher value of and a lower driving force for the first stage of austempering at a fixed austempering temperature [13]. In other words, the nucleation of ferrite plates is more difficult and a slower kinetics is expected. This is clearly highlighted in Figure 5, showing the initial portion of the dilatometric curves. On the other side, this result may be also explained in view of the transformation mechanisms, involving the diffusion of C from the ferrite region towards the neighbor austenite, which is clearly obstructed if the parent austenite is reacher in C. The activation energy related to this transformation was calculated as indicated in the experimental procedures. The linear trend for the experimental points associated to the austempering experiments at 850°C confirms that the process can be described by a single activation energy value equal to 23,95KJ/mol. It is not the case for the experimental points associated to the higher austenitizing temperature, which show a change of slope by changing austempering temperature. In the low temperature range (<320°C) the activation energy was 26,0KJ/mol, not much different from that calculated at 850°C. Indeed, the activation energy decreased to 6.0KJ/mol in the high temperature range, similarly to previous findings [8].

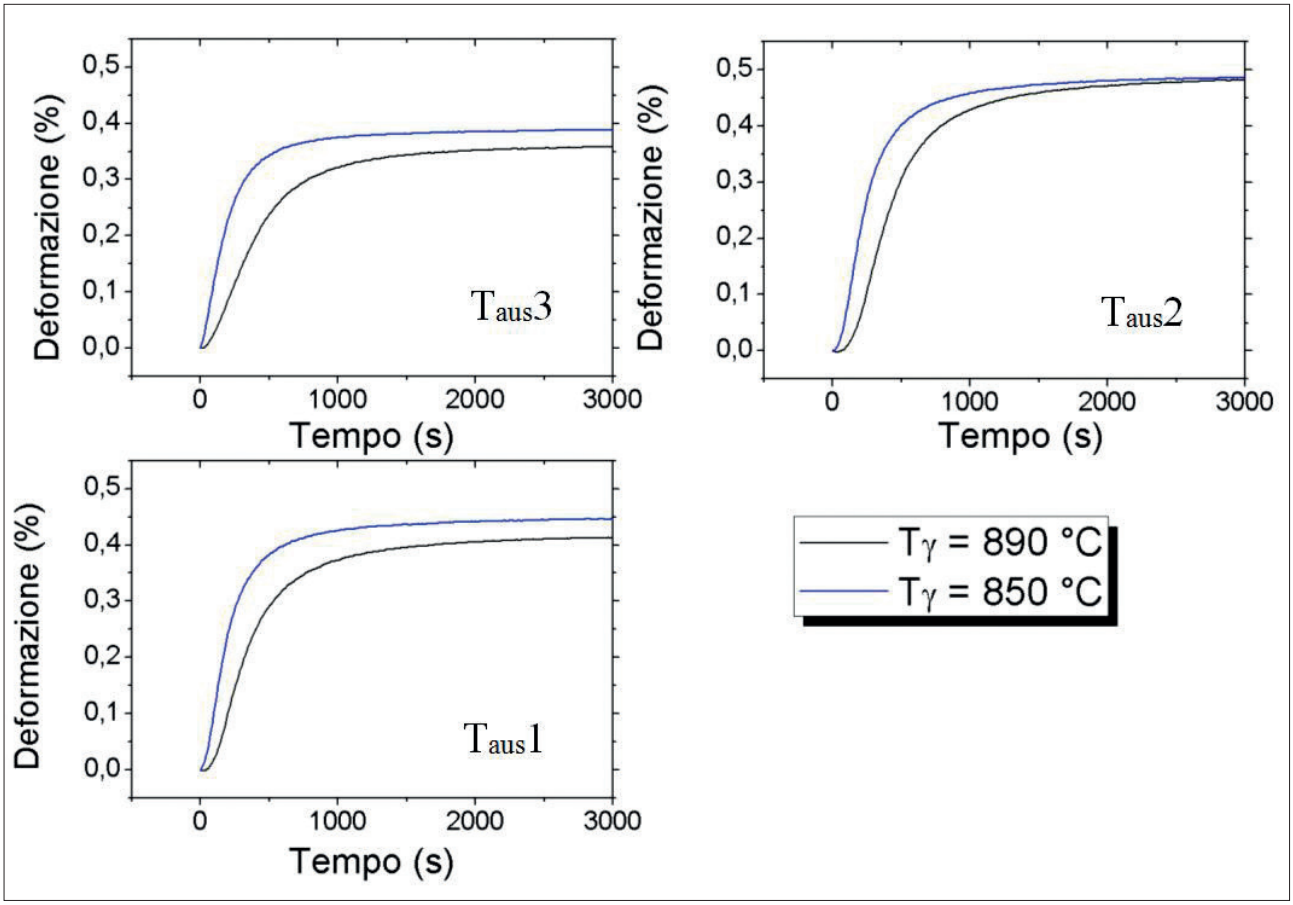

Fig. 5 - influence of the austenitizing temperature on the austempering kinetics

A first general comment to the activation energy values is that these are relatively low compared to those reported in literature (40-70KJ/mol) in the austenitizing temperature range used in this work [3,14]. On the other side, present values are higher than those reported in [8]. Nevertheless, the chemical composition plays a fundamental role with this respect and a more systematic analysis would be required to highlight the influence of alloying elements.

Concerning the different values for samples austenitized at 850 and 890°C it is thought that the reason lies in the coarser microstructure observed at higher temperature, in agreement with the larger parent austenite grain size (Figure 7). At 850°C the grain size is smaller and the formation of ferrite plates is thus expected to saturate the neighbor austenite at an earlier stage of the process, in good agreement with previous dilatometric results. The transformation mechanisms does not change for different austempering temperature, meaning that the kinetics is unchanged between 290 and 400°C. On the other hand, the grain size is bigger is samples austenitized at 890°C and the C saturation of austenite becomes more difficult, particularly at high austempering temperature, when the diffusion of C is faster. Accordingly, the transformation can proceed with a faster kinetics, as confirmed by the low activation energy. A similar trend was previously claimed by Dorazil, who reported a lower activation energy for the formation of upper bainite, at high austempering temperature, compared to lower bainite [3].

At lower austempering temperature, when the diffusion of C is slower, saturation can occur even in coarse grained austenite and the activation energy is thus similar to that observed in the fine grained material. The proposed explanation well fits with recent findings, showing that while at higher austempering temperatures C redistribution takes place almost parallel to the (i) phase transformation, at 300°C the redistribution of carbon to austenite lags behind considerably [15].

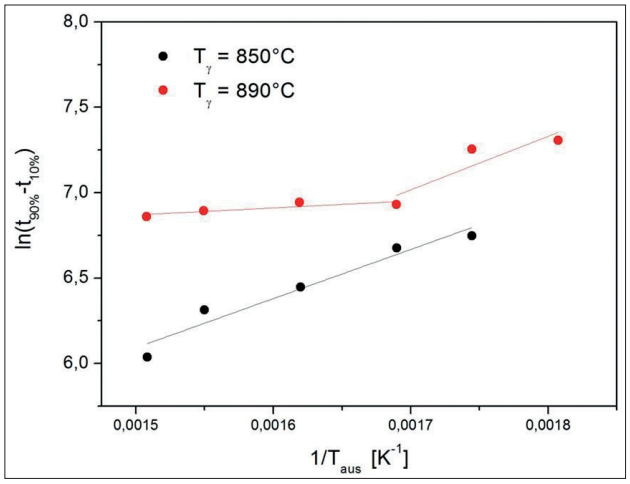

Fig. 6 - Calculation of the activation energy

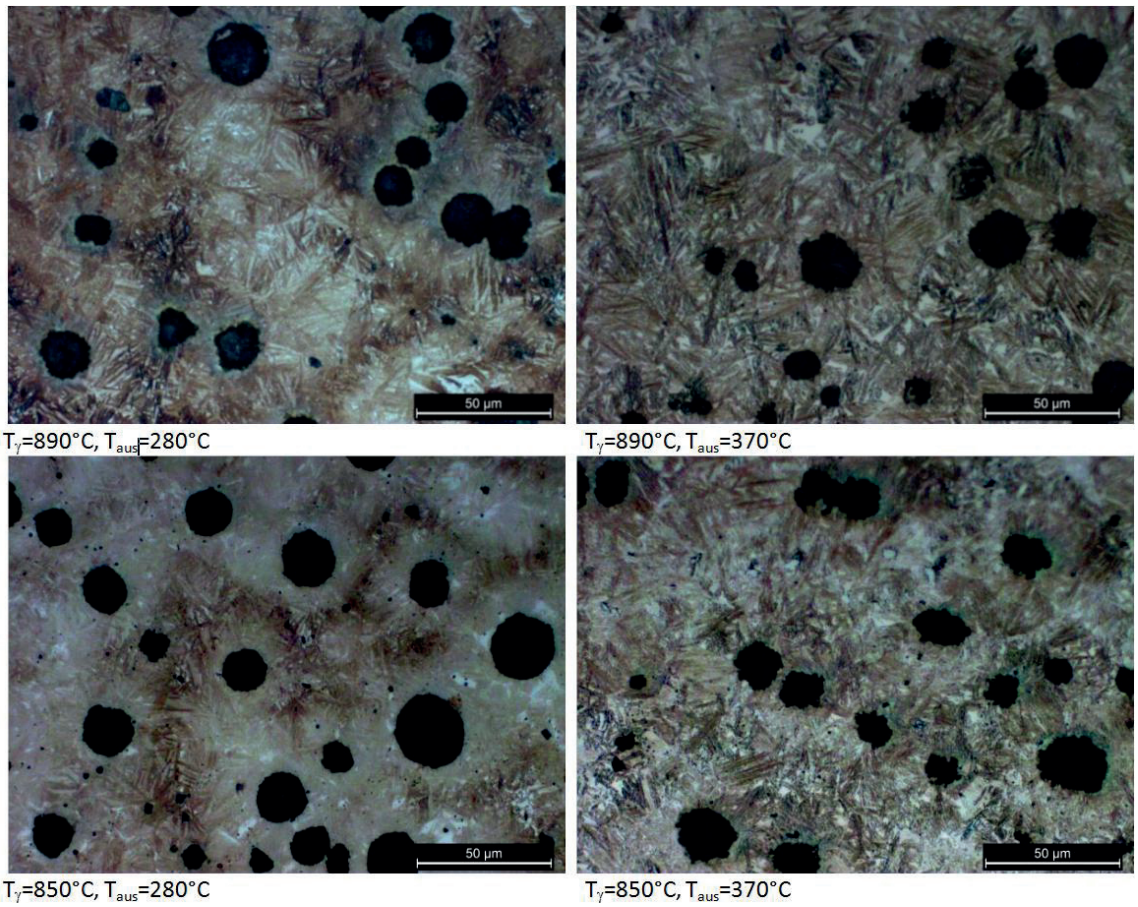

Fig. 7 - Microstructure of samples austempered at 280 and 370°C after austenitizing at different temperature

Beneath the considerations regarding the grain size, the micrographs in Figure 7 are in good agreement with dilatometric tests results.
The amount of retained austenite decreases by decreasing austempering temperature and is generally higher in samples austenitized at 890°C. As expected, the size of bainitic ferrite is larger in coarse grained microstructure.
A lower bainite morphology is found up to 320°C, increasing fraction of upper bainite being observed at higher temperature.

CONCLUSIONS

The influence of austenitizing temperature on the austempering kinetics of an austempered ductile iron was studied by dilatometry.
The first stage of transformation, involving the decomposition of austenite into ferritic bainite and C enriched austenite is associated to a net expansion, whose extent is proportional to the fraction transformed.
The higher austenitizing temperature (890°C) caused a slower transformation kinetics, due to the lower driving force associated to the higher C content in austenite.
For the same reason, a lower austempering temperature caused a higher degree of transformation. At 850°C the activation energy of the transformation was about 24KJ/mol and did not change inside the investigated range of austempering tempertures.
A similar value of activation energy was determined at 890°C, when the austempering temperature was below 320°C.
At higher temperature the activation energy dropped to 6KJ/mol in view of the slower C saturation of coarse grained austenite and the easier formation of ferrite.
Dilatometric results are in good agreement with microstructure of austempered samples.

REFERENCE

[1] R. B. GUNDLACH and J. F. JANOWAK, Met. Prog. 128, (1985), p. 19-28.
[2] J. R. DAVIS, "Cast Irons", ASM international (1999)
[3] E. DORAZIL, "High Strength Austempered Ductile Cast Iron", Ellis Horwood, (1991)
[4] N.DARWISH, R. ELLIOTT, Materials Science and Technology 9 (1993), pp. 572-585
[5] S. YAZDANI, R. ELLIOT, Materials Science and Technology 15, (1999), pp. 896-902
[6] J. M. VELEZ, A. GARBOGGINI, AND A. P. TSCHIPTSCHIN, Materials Science and Technology 12, (1996) pp. 329-337
[7] E. FRAS, M. GORNY, E. TYRALA, H. LOPEZ, Materials Science and Technology 28 (2012), pp. 1391-1396
[8] M. M. CISNEROS-GUERRERO, R.E. CAMPOS-CAMBRANIS, M.J. CASTRO-ROMÀN E M.J. PÉREZ-LÒPEZ, Advanced Materials Research 4-5, (1997), pp. 415-420
[9] M. J. PÉREZ, M. M. CISNEROS, E. ALMANZA E S. HARO, Journal of Materials Engineering and Performance 21, (2012),pp. 2460-2466
[10] ASTM International E2567 (2013) - standard test method for determining nodularity and nodule count in ductile iron using image analysis"
[11] E. J. MITTEMEIJER, J. Mat. Science 27, (1992) p. 3977.
[12] L. C. CHANG, Metallurgical and Materials Transactions 34A, (2003), pp. 211-217
[13] N.DARWISH, R. ELLIOTT, Materials Science and Technology 6, (1993), pp. 586-602
[14] M. NILI AHMADABADI AND S. FARJAMI, Materials Science and Technology 19, (2003) p. 645
[15] L. MEIER , M. HOFMANN, P. SAAL , W. VOLK, H. HOFFMANN, Materials Characterization 85, (2013), pp.124 - 133